Macromolecules

ARTICLE

pubs.acs.org/Macromolecules

Hydrodynamic Properties of Wormlike Macromolecules: Monte Carlo Simulation and Global Analysis of Experimental Data

D. Amorós, A. Ortega, and J. García de la Torre*

Departamento de Química Física, Facultad de Química, Universidad de Murcia, 30071 Murcia, Spain

Supporting Information

ABSTRACT: A Monte Carlo simulation, coupled with bead-model hydrodynamic calculation, has been employed to predict hydrodynamic coefficients and other solution properties, of wormlike macromolecules, covering the full range of the wormlike model, from short cylinders to very long, fully flexible chains, eventually including excluded-volume effects. The results have been implemented in a computational tool, Multi-HYDFIT, which performs the determination of the structural parameters from a set of experimental data of various properties for multiple samples with varying molecular weight. An analysis of experimental data of double-stranded DNA demonstrates that the Multi-HYDFIT treatment, with our simulation results, predicts the various solution properties of DNA in an extremely wide range of sizes, from 8 to 200 000 base pairs, yielding values of the parameters that agree with those of the double helix. The scheme is also applied to other synthetic and biological macromolecules, like the very stiff, triple-helical schizophyllan polysaccharide or the very flexible poly(isobutylene) polymer, the latter covering again an extremely wide range that includes quite short oligomers.

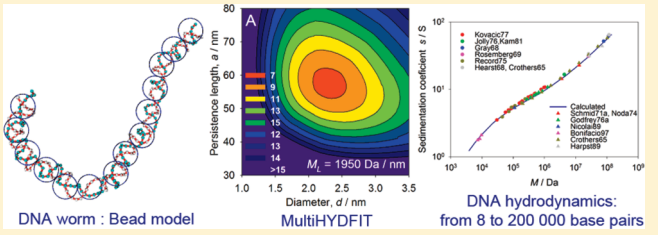

INTRODUCTION

There is a variety of synthetic polymers and biological macromolecules which possess a semiflexible skeleton and can be properly represented by the wormlike chain model.[1] According to standard terminology, the wormlike chain is used to represent: "a hypothetical linear macromolecule consisting of an infinitely thin chain of continuous curvature; the direction of curvature at any point is random. The model describes the whole spectrum of chains with different degrees of chain stiffness from rigid rods to random coils, and is particularly useful for representing stiff chains. In the literature this chain is sometimes referred to as a Porod−Kratky chain".[2]

The wormlike model is particularly relevant for biopolymers. Double-stranded DNA is a paradigmatic example,[3,4] but there are other most useful applications, like polysaccharides (see for instance refs 5 and 6). About 30 years ago, Yamakawa and Fujii presented a theoretical treatment of the solution properties of the wormlike model.[7−9] Their treatment included several assumptions, the most serious of which were the approximation of replacing the Oseen tensor by its preaveraged value and, for its application to very long chains, the absence of excluded-volume effects. It has been shown that this approximation introduces appreciable errors for both rigid straight chains[10] and random coils.[11] On the other hand, Zimm and others[12−14] proposed to calculate hydrodynamic properties of flexible macromolecules by the Monte Carlo rigid-body method. This method is inspired by the pioneering work of Kirkwood and Riseman,[15] who modeled macromolecules as strings of beads. In the rigid-body treatment, conformations of the chain are generated by a Monte Carlo procedure. For each conformation, the properties are individually computed using hydrodynamically rigorous procedures,[16] and the final values are the conformational averages. This treatment has been shown to predict correctly experimental results for fully flexible random-coil polymers in both ideal and good solvent conditions.[11,17,18]

The rigid body Monte Carlo treatment was first used for wormlike chains by Hagerman and Zimm[13] in their study of the rotational dynamics of short or moderately long DNAs, whose conformation looks like a weakly bending rod. This work was extended to other solution properties (translational dynamics and intrinsic viscosity) by Molina et al.[19] The procedure suffered from the important computational cost required to obtain the various properties for highly flexible chains with a large number of beads, and the applicability of the procedure was restricted by the limited computing power available by those years. More recently, an alternative approach, the numerical path-integration method applied to a wormlike cylinder, has been presented and used to interpret data of moderately long DNA molecules.[20] In the present paper, we present a new Monte Carlo simulation study of the solution properties of wormlike chains which benefits of recent advances in macromolecular hydrodynamics. Thus, bead model calculation is done with the latest version of the HYDRO methodology,[21] and the handling of numerical results and experimental properties is facilitated using equivalent radii and ratios of radii.[22] The calculation covers the full range of the wormlike chain model, from short, thick, rigid cylindrical

Received: November 26, 2010
Revised: February 3, 2011
Published: June 21, 2011

particles to fully flexible random coils. The relevance of such wide coverage is illustrated in the analysis of experimental data for DNA—the paradigmatic wormlike macromolecule—covering an extremely wide range of sizes, from 10 to 10^5 base pairs. Our methodologies also facilitate the analysis of experimental data using the Multi-HYDFIT tool,[22] in which our simulation results have been implemented. We show how this easy and effective tool allows an immediate fit of various solution properties of DNA over such wide range of molecular weight, yielding very precisely the wormlike parameters of the double helix.

MODELS AND SIMULATION

The Wormlike Chain. The original Kratky−Porod wormlike chain is a continuous filament having a contour length L and a diameter d. The parameter that measures the degree of flexibility is the persistence length, a, and the conformation presented by the chain is determined by the ratio $X = L/a$. The chain looks like a slightly bending rod if X is small, with the limit of the straight rod corresponding to $X \rightarrow 0$, while when X is large the model is close to the random-coil model, which holds in the limit $X \rightarrow \infty$. Thus, it is not a, but the ratio X what determines the conformation of the wormlike chain.

The mean square end-to-end distance of the wormlike chain was originally derived by Kratky and Porod[1]

$$\langle r^2 \rangle = 2aL\left[\left(1 - \frac{1}{X}\right)\left(1 - e^{-X}\right)\right] \quad (1)$$

and the mean-square radius of gyration, $\langle s^2 \rangle$ (we employ the short-hand notation $R_g^2 \equiv \langle s^2 \rangle$), of an infinitely thin wormlike chain, without excluded volume effects, was derived years later by Benoit and Doty (BD):[23]

$$R_{g,BD}^2 = 2aL\left[\frac{1}{6} - \frac{1}{2X} + \frac{1}{X^2} - \frac{1}{X^3}\left(1 - e^{-X}\right)\right] \quad (2)$$

The cross section of the filament is assumed to be uniform and circular, so that the chains looks like a curved cylinder of (hydrodynamic) diameter d. In the limit of $X \rightarrow 0$, the model is a right cylinder with length-to-diameter ratio $p = L/d$.

Rather than the contour length L, the size of the chain is expressed by the molecular weight, M. The mass per unit length, $M_L = M/L$, a, and d are the characteristic structural parameters of a wormlike macromolecule.

Rigid-Body Monte Carlo Approach and Bead-Model Calculations. As it has been described in the Introduction, the properties will be calculated from a Monte Carlo simulation, in terms of the rigid-body treatment of flexible entities, in which the properties are obtained as conformational averages over the properties evaluated for individual conformations that are considered as instantaneously rigid particles. The procedure requires rigid-body hydrodynamic calculation which will be made on bead models of the wormlike chain, constructed as described below. For such calculation we use advanced methodology embodied in bead-model hydrodynamics[24−26] and in the new HYDRO++ computational tool.[21] Of the various new approaches intended to improve the calculation of rotational coefficient and intrinsic viscosity, we pay special attention to the latter, which in the present work is obtained with the so-called adjusted volume correction.[21,27]

For the purpose of handling the results of the Monte Carlo simulation—in regard to both their dependence on structural parameter and their use in the determination of such parameters from experimental data—we have found very useful the employment of the concepts of equivalent radii and ratios of radii.[22] The equivalent radii are the values of the radius of a spherical particle that would have a given value of some property. For the solution properties considered in this work, namely the radius of gyration, R_g, the translational diffusion, D_t, or, equivalently, the sedimentation coefficient, s:

$$s = \frac{D_t M(1 - \bar{v}\rho)}{N_A k_B T} \quad (3)$$

and the intrinsic viscosity $[\eta]$, the equivalent radii are defined as[22]

$$a_G = \sqrt{\frac{5}{3}} R_g \quad (4)$$

$$a_T = \frac{k_B T}{6\pi\eta_0 D_t} \quad (5)$$

$$a_I = \left(\frac{3M[\eta]}{10\pi N_A}\right)^{1/3} \quad (6)$$

In the preceding equations, η_0 is the solvent viscosity, $\bar{v}$ is the partial specific volume of the macromolecule, M is its molecular weight, ρ is the solution density, T is the absolute temperature, and k_B and N_A are the Boltzmann and Avogadro constants. The a_G, a_T, and a_I radii do not depend on these quantities; they depend only on the size and conformation of the macromolecular solute, which in the case of the wormlike chain are determined by the three parameters L, a, and d. The equivalent radii can be, in turn, combined into ratios of radii:

$$GT = \frac{a_G}{a_T} = \frac{6\pi\eta_0 D_t}{k_B T}\frac{R_g}{(3/5)^{1/2}} = \frac{6\pi\eta_0 N_A s}{M(1 - \bar{v}\rho)}\frac{R_g}{(3/5)^{1/2}} \quad (7)$$

$$GI = \frac{a_G}{a_I} = \left(\frac{10\pi N_A}{3[\eta]M}\right)^{1/3}\left(\frac{5}{3}\right)^{1/2} R_g \quad (8)$$

$$IT = \frac{a_I}{a_T} = \frac{GT}{GI} = \left(\frac{3[\eta]M}{10\pi N_A}\right)^{1/3}\left(\frac{k_B T}{6\pi\eta_0 D_t}\right) \quad (9)$$

The ratios of radii do not depend on the absolute size but only on the shape or conformation of the solute. In the case of the wormlike chain, these GT, GI, and IT ratios are functions of the quantities that determine their conformation, which are the ratios of parameters, L/d and L/a (or any combination of these parameter ratios), but not on the individual values of L, a, and d. Thus, in our Monte Carlo calculations, we shall assign an arbitrary value to any of these length parameters (for instance d = 20 Å), and the values of the two others are varied in a convenient manner (vide infra). The results for R_g, D_t, and $[\eta]$ are recast in the form of GT, GI, and IT ratios, whose dependence on the ratios L/d and L/a (or any function of them) will not depend on the choice of d, but instead they will have an universal validity, being applicable to any wormlike chain.

The Schellman−Hagerman−Zimm Model. Our model for the wormlike chain is that originally proposed by Hagerman and Zimm,[13] based on an original idea by Schellman[28] (hereafter denoted as the SHZ chain). This model was already used in our

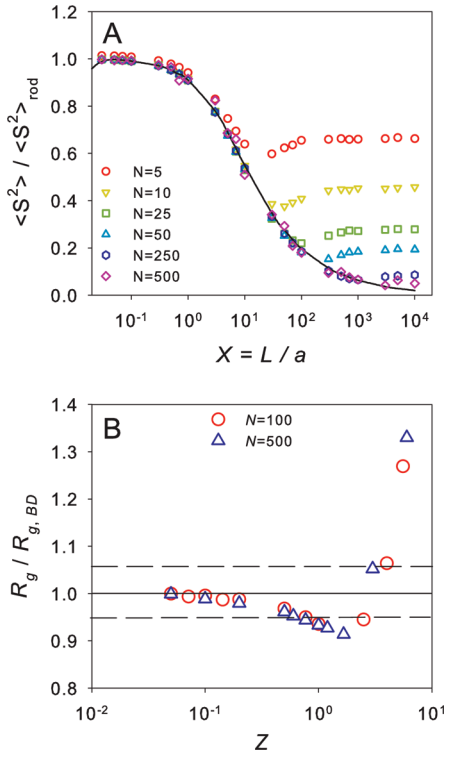

Figure 1. (A) Mean-square radius of gyration of wormlike chains, normalized to that of a rigid, straight rod of the same contour length. Simulation results for the Schellman−Hagerman−Zimm chain and results from the exact Benoit−Doty formula. (B) Ratio of the simulation results for $N = 10$ and 500, to the exact result.

above-mentioned previous study.[19] The contour of a continuous wormlike chain is discretized as a polygone having N elements joined by $N - 1$ connectors of fixed length b; therefore, the contour length is $L = (N - 1)b$. The angle between consecutive connectors, θ, is a random variable. In the Monte Carlo generation of individual conformations of the chain, each of the $N - 2$ angles is generated as the composition of two angular displacements

$$\theta = (\theta_1^2 + \theta_2^2)^{1/2} \tag{10}$$

where the θ_1 and θ_2 angles are normally distributed random numbers with zero mean and a standard deviation equal to $(b/a)^{1/2}$. The torsional angles, ϕ, are random numbers with uniform distribution in $(0, 2\pi)$. In the Monte Carlo simulation, the conformations are generated obtaining the bead coordinates sequentially: from the coordinates of elements $i - 3$, $i - 2$, and $i - 1$, those of bead i are obtained, using standard methods,[29] from the values of the angle θ corresponding to the $(i - 2, i - 1, i)$ trio and the internal rotation angle ϕ corresponding to the $(i - 2, i - 1)$ bond, generated as random number with the indicated statistics.

From the coordinates, properties of the individual conformations (to be used in the Monte Carlo averages) can be evaluated. Thus, the radius of gyration can be obtained easily from

$$R_g^2 = \frac{1}{2N^2}\sum_{i=1}^{N}\sum_{j=1}^{N}\langle r_{ij}^2\rangle \tag{11}$$

where $\langle r_{ij}^2\rangle$ is the mean-square distance between beads i and j.

A previous analysis of the R_g^2 values is most useful to check the simulation results by comparison with the exact, theoretical expression derived by Benoit and Doty (eq 2). Thus, we simulated ensembles of 2000 conformations of chains with varying N and a. Results are plotted in Figure 1A (normalized to the rigid-rod value, $R_g^2(\text{rod}) = L^2/12$ which is the $X \to 0$ limit of the BD expression). We see that the simulation results for Schellman−Hagerman−Zimm follow well the theoretical expression up to some value of the X parameter. Thus, for $N = 500$, the validity ceases for $X \approx 100-1000$. The results for various N suggest that the limiting X is proportional to N, so that the validity of the SHZ model can be assured up to a limit of the parameter

$$Z = \frac{X}{N} = \frac{b}{a} \tag{12}$$

This fact is confirmed in Figure 1B, where the ratio of the simulated R_g to the exact value from the BD formula is displayed, as a function of Z, for two widely different chain lengths, $N = 100$ and $N = 500$, for which the trend is identical. Accepting differences within 5% in R_g (ratios from 0.95 to 1.05), we notice that the simulations with the SHZ chain reproduce well the exact results up to $Z \approx 1$. Fortunately, this range covers all cases of interests. Clearly, it covers the case of stiff macromolecules; for instance, B-DNA, whose wormlike chain parameters are (as it will be confirmed in our results) $a \sim 500$ Å and $d \sim 20$ Å, with $b \sim 25$ Å (vide infra) the quotient is $Z = b/a \sim 0.05$. For a extremely stiff polysaccharide, namely schizophyllan, $a \sim 2000$ Å and $d \sim 25$ Å, with $Z \sim 0.015$.[30] At the other extreme, we would find cases like thick wormlike micelles, with $Z \sim 0.1$, and even the most flexible polymers, like polystyrene, with $a \sim 15$ Å, $d \sim 7$ Å,[31,32] and $Z \sim 0.6$, that are covered within the range of our calculation.

Wormlike Chains near the Rod Limit. The representation of the cross section of the wormlike filament is most relevant near the rod limit, for small values of parameter X. In the Hagerman−Zimm[13] hydrodynamic version of the Schellman chain,[28] the filament with uniform circular cross section of diameter d is represented as a string of touching beads, whose diameter, b, is the same as the length of the bonds joining neighbor elements in the Schellman chain. The hydrodynamic radius of the beads, to be used in the HYDRO calculation, would then be $\sigma = b/2$. Hagerman and Zimm proposed to take a value of b so that the volume of the string of beads would be the same as that of the cylinder, which gives the relationship

$$d = \sqrt{2/3}b = 0.8165b \tag{13}$$

Thus, the length-to-diameter ratio, in the cylindrical wormlike filament is related to the number of beads in the chain by

$$p = L/d = N/\sqrt{2/3} = 0.8165N \tag{14}$$

The replacement of the cylindrical filament by the string of beads may introduce some bias that could be appreciable for short chains. Although the volume equivalence between the diameters of the cylinder and the bead, as formulated in eq 13, minimizes the difference, there could be some additional difference arising from hydrodynamic effects. Such differences were found in our earlier study,[19] comparing the results of a straight rod of beads with those of a cylinder. In this work we employ an advanced version of bead-model calculations[21] which improves the calculation of diffusion coefficients and

Table 1. Ratios of the Properties of a Straight String of Touching Beads of Diameter d, with Length $L = Nb$, to Those of a Cylinder of Length L, Diameter $d = 0.8165b$ and Aspect Ratio $p = 1.225N$

N	p	R_g(chain)/R_g(cyl)	D_t(chain)/D_t(cyl)	$[\eta]$(chain)/$[\eta]$(cyl)
1	1.225	0.949	1.014	0.883
2	2.449	0.979	1.029	0.928
3	3.674	0.990	1.014	0.946
4	4.899	0.994	1.011	0.973
5	6.124	0.996	1.009	0.974
7	8.573	0.998	1.006	0.961
10	12.247	0.999	1.001	0.957
15	18.371	1.000	0.990	1.001
20	24.495	1.001	0.997	1.002

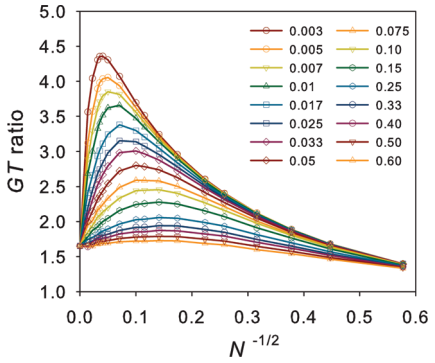

Figure 2. GT ratio plotted vs $N^{-1/2}$ for wormlike chains with the indicated values of Z. The intercept is the result for fully flexible random coils.

the intrinsic viscosity. (The square radius of gyration is also corrected for finite bead size adding the term $3b^2/20$, which is the square radius of gyration of a bead of diameter b.) Then, comparing now the results for straight strings of beads and circular cylinders, we find that the differences are quite small even for the shortest rods. Table 1 reports for the radius of gyration, translational diffusion, and intrinsic viscosity, the ratio of the property of the cylinder to that of the rod of beads having the same length L and volume-equalized diameters d and b. The results extend through the range, up to $p = 20$, of our results[33] for cylinders. With all the ratios so close to unity, it is clear that the cylinder and the volume-equalized rod of beads are practically equivalent in their hydrodynamic properties. We have also verified (results not shown) that in the limit of very large L or N the properties of the bead of rods, calculated with the advanced hydrodynamics, coincide with those of long cylinders, available from classical theories.[34−37] We assume that this equivalence between the two rigid, straight models holds for the flexible wormlike and bead chains. This seems reasonable for partially flexible chains with moderate L/a, and we do not worry about what happens in the limit of long, fully flexible coils because in such limit the solution properties are practically independent of the chain cross section. In summary, the properties for the wormlike chain with diameter d will be those evaluated for the SHZ chain of touching beads of diameter $b = 1.225d$.

In our Monte Carlo simulations, we varied the number of beads in the range $N = 2-5000$, with the upper limit dictated by the computing cost of the hydrodynamic calculations, that require CPU time proportional to N^3. We also varied the conformations of the wormlike chains within the range $Z = 0-0.6$ which, as described above, assures the validity of the Schellman−Hagerman−Zimm model for any value of N. From any pair of N and Z, the corresponding parameters of the wormlike chain are, according to eqs 12 and 13, $L = Nb$, $a = b/Z$, and $d = 0.8165b$, and they determine the b/a and $\sigma = b/2$ values used in the Monte Carlo rigid-body calculation of properties. The results are then put into the form of GT, GI, and IT values, whose dependence on N and Z is, as indicated above, independent of the d value used in the simulation and then of universal validity for any wormlike chain. A list of numerical values is given in Table S-1 (Supporting Information). The GT ratio is plotted vs N and vs Z in Figure 2. The plot of GI (not shown) is very similar; indeed, the GI values are quite close to those of GT (except for very long and rigid rods), with IT being close to unity (as it happens for a variety of rigid and flexible macromolecules, as demonstrated in ref 22). For reasons that will be apparent later, for the dependence on the number of elements, N, we have used $1/\sqrt{N}$ instead of N itself. Plots of the GI and IT ratios are presented in the Supporting Information.

In the Monte Carlo simulation, the number of generated conformations was divided into five subsamples. The final value was the mean of the five values for each subsample, and from their standard deviation the statistical error of the properties was determined and used to find the errors of the ratios of radii GT and GI, which were in all cases smaller than 5%.

The advantage of using ratios of radii for the presentation and handling of the values of the physical properties (additional to their independence on the absolute sizes) is evident in Figure 2 and Table S-1. While the various solution properties have a strong dependence on the absolute parameters, the dependence of the ratios of radii on the relative parameters (here N and Z) is quite weak and smooth. Over wide ranges of conformations of the wormlike chain, all the ratios of radii are of the same order of magnitude, varying, roughly, from 1.5 to 4 in the case of GT and from 1.5 to 2.5 in the case of GI.

The thickness of the wormlike chain has a slight influence on its radius of gyration, which would be somehow larger than that of the infinitely thin filament. Clearly, such influence must vanish for very long chains, regardless of their more or less rigidity, in the limits of $N \rightarrow \infty$. Our calculation for the string-of-beads representation of the SHZ chain accounts for the effect of finite bead size on the radius of gyration adding the term indicated above. This effect, along with the marginal effect of the discretization, is expressed in the form of a ratio $RR = R_g/R_{g,BD}$, where $R_{g,BD}$ is the BD value. The ratios are listed in Table S-1, where we appreciate that they are quite close to unity, being closer for higher N, as expected.

Wormlike Chains near the Random Coil Limit. The range of wormlike chains covered in the range $N \leq 5000$ is quite wide; for instance, in the case of B-DNA with the well-known structural data (which will be confirmed later on in this paper) $M_L \approx 200$ Da/Å and $d \approx 20$ Å (or $b = 25$ Å), this is tantamount to $M < 20 \times 10^6$ Da, i.e., up to about 30 000 base pairs.

Regardless of the inherent rigidity of the chain, measured by the persistence length, a, in the limit of very long chains, $L/a \rightarrow \infty$, and $N \rightarrow \infty$, the wormlike chain reduces to the fully flexible, random coil chain, whose statistical and hydrodynamic properties are well-known. For random coils, the radius of gyration has

dx.doi.org/10.1021/ma102697q |Macromolecules 2011, 44, 5788–5797

been customarily related to the hydrodynamic properties by means of the so-called Flory constants:[38,39]

$$P_0 = \frac{f}{\eta_0 \langle r^2 \rangle^{1/2}} \tag{15}$$

and

$$\Phi = \frac{[\eta] M}{\langle r^2 \rangle^{3/2}} \tag{16}$$

Recalling that, for the random coil, $R_g{}^2 = \langle r^2 \rangle / 6$, one immediately finds that the Flory constants and our ratios of the hydrodynamic radii to the radius of gyration are simply related by $P_0 = 9.93/GT$ and $\Phi = 9.23 \times 10^{23}/GI^3$. The accurate determination of the Flory universal random-coil constants has been the subject of numerous works. Monte Carlo rigid-body calculations, as proposed by Zimm,[12] carried by García de la Torre and coworkers,[11] yielded $P_0 = 6.0$ and $\Phi = 2.5 \times 10^{23}$, results that were found to be in excellent agreement with experimental data of the extremely well characterized polystyrene/cyclohexane/35 °C system[40−42] Then, the corresponding values of our ratios for fully flexible random coils are $GT = 1.65$ and $GI = 1.53$.

As these values correspond to the $N \rightarrow \infty$ limit for any value of Z, they should be the extrapolated intercept of the values with finite N. It has been noted that, in order to extrapolate results for discrete models of random coils, a convenient variable is $1/\sqrt{N}$. In Figure 2, which shows the variation of the GT ratio, we see how the numerical values extrapolate neatly to the expected limit. The situation is completely similar for the GI ratio, whose plot has indeed the same aspect.

Excluded Volume. Excluded volume (EV) effects are influential in the solution properties of long flexible polymers. The combined influences of chain length and flexibility are usually expressed by the number of statistic (Kuhn) segments, $L/(2a) = X/2$. Many polymers to which the wormlike model is applied have either (or both) large rigidity a, or short contour length, so that the number of Kuhn segments is not too large and excluded volume effects can be safely ignored.

Nonetheless, as we intend that our treatment will cover the flexible coil limit of the wormlike model, including very long and very flexible macromolecules, we have introduced EV effects in a simple manner that can cover those less frequent cases. The rigid-body Monte Carlo simulations of the SHZ chain were carried out with the restriction that the generated chains would be free of overlap; chains in which the distance between any pair of beads was smaller than the diameter b were rejected. Using the hydrodynamic diameter as the parameter in the hard-core excluded-representation limits the applicability of our results to cases when intramolecular electrostatic repulsions (which would be present in long polyelectrolyte chains if ionic strength is not sufficiently high) could be safely ignored. An alternative would be using a different, effective hard-core diameter that would be larger than b as to represent the additional electrostatic repulsion. Such approach has been shown to be equivalent to a detailed Debye−Hückel description of the double-layer repulsion.[43−45] However, this could add one more parameter to the three that we are already considering, M_L, a and d, thus adding much more complexity to our simulation and, mostly, to the data analysis procedures.

This restricted the reach of our calculations to $N \leq 500$ for the largest Z (most flexible chains). The GT and GI values computed with EV were just slightly higher than those without EV, and the aspect of their variation with N and Z was quite similar. Results are listed in Table S-2 and plotted in Figure S-2 (Supporting Information).

In the flexible chain limit, the consensus values of the Flory parameters P_0 and Φ, obtained in the rigid-body Monte Carlo simulation,[18] in agreement with experimental data of the well characterized systems polystyrene/ethylbenzene/25 °C[46,47] and polystyrene/toluene/20 °C, when transformed into ratios of radii give[22] $GT = 1.87$ and $GI = 1.69$. These are the values to be used as the $N \rightarrow \infty$ or $N^{-1/2} = 0$ limit instead of those indicated above when EV is absent.

While the trend and handling of the GT and GI ratios does not present any peculiarity (apart from the numerical differences), the radius of gyration, relative to the non-EV value reflects the typical chain expansion, which is usually characterized by the expansion factor:

$$\alpha_g{}^2 = R_{g,EV}{}^2 / R_g{}^2 = \langle s^2 \rangle_{EV} / \langle s^2 \rangle \tag{17}$$

Note that we use the EV subscript for quantities with EV and omit any subscript in the non-EV case.

The theory of EV effects is particularly complex in the case of semiflexible chains. In most applications of the wormlike chain model the EV effect may not be appreciable; indeed, it will be intense enough only for very long and very flexible chains. Thus, we have adopted a simple description to handle such cases. For very long chains, $R_g \propto N^{1/2}$ and $R_{g,EV} \propto N^{\nu}$, with $\nu \approx 0.6$, a more precise value being $\nu = 0.585$,[48,49] which gives

$$\alpha_g{}^2 = QN^{0.17} \tag{18}$$

The numerical term Q would depend on the strength of the EV effect which in our model is gauged by the bead diameter, which is the hard-spheres EV parameter. Using our R_g and $R_{g,EV}$ Monte Carlo results, we have evaluated $\alpha_g{}^2$ and the numerical values of $Q = \alpha_g{}^2/N^{0.17}$, which are reported in Table S-2 (Supporting Information). For our finite chains, this value has a slight dependence on N and should extrapolate to some value Q_∞ for infinite N. Indeed, the extrapolation is well linear in a plot vs $N^{-1/2}$, shown in Figure S-3 (Supporting Information) where the Q_∞ values are obtained as the intercepts. The extrapolated values are included in Table S-2. As expected, the Q values for a given N decrease with decreasing $Z = b/a$, as they should, because they should decrease when the hard-spheres diameter d is decreased. With our numerical values, we empirically find a power law $Q_\infty = 0.84Z^{0.48}$. This suggests $Q_\infty \propto Z^{1/2}$, although we have not pursued further these dependence because, as mentioned, the EV problem has a marginal importance in our work.

■ ANALYSIS OF EXPERIMENTAL DATA

Prediction of Physical Properties. With the results from the computer simulation, for the ratios GT, GI, and RR, the physical solution properties of a wormlike molecule with given values of L, a, and d are obtained as follows. First, these parameters are used to obtain $R_{g,BD}$, and they are next transformed into the quantities $b = d/0.8165 = 1.225d$, $Z = b/a$, and $1/\sqrt{N} = (b/L)^{1/2}$. By interpolation in Table S-1, we determine the GT, GI, and RR ratios corresponding to those N and Z. Commenting again on the utility of the ratios of radii, we note that the interpolation is greatly facilitated by their weak and smooth variation over the whole range of the wormlike chain parameters. From RR, we first evaluate $R_g = RR \times R_{g,BD}$, and a_G from eq 4, then, the equivalent

radii, $a_T = a_G/GT$ and $a_I = a_G/GT$, are obtained, and finally D_t and $[\eta]$ are obtained from eqs 5 and 6, the latter requiring the value of the molecular weight or that of the relative parameter M_L.

If the excluded volume effect is considered, then the results in Table S-2 are employed. The value of R_g is expanded with the Q factor, obtaining $R_g = QN^{0.17}R_{g,BD} \times RR$, and D_t and $[\eta]$ are determined with the GT and GI ratios listed in Table S-2.

Sedimentation coefficients, s, are derived from diffusion coefficients by means of the well-known Svedberg equation

$$s = \frac{M(1-\bar{v}\rho)}{RT} D_t \tag{19}$$

where $\bar{v}$ is the partial specific volume of the solute and ρ the solution density.

Determination of Wormlike Chain Parameters from Experimental Data. The ultimate goal of studying the wormlike model should be to provide a protocol to extract the structurally relevant information, contained in parameters like a, M_L, and d, from experimental data. Usually, experimental values of the solution properties are available for a series of samples with varying molecular weight. In order to analyze simultaneously several properties of various samples, in a search for structural parameters, in a previous paper[22] we described a strategy, implemented in the Multi-HYDFIT computer program, which again is based on equivalent radii.

Let us denote Y any of the observable properties, R_g, D_t, s, $[\eta]$, etc. As we have just described, our results allow the prediction of these properties as functions of molecular weight from given values of the parameters. In the Multi-HYDFIT strategy, the properties are transformed into equivalent radii, a_Y, which are considered functions of molecular weight, with a dependence that in turn depends on the model parameters. In the case of the wormlike chain, this can be expressed as $a_{Y(\mathrm{cal})}(M;a,M_L,d)$. Then, the Multi-HYDFIT procedure optimizes the parameters seeking the minimization of a target function such as

$$\Delta^2(a,M_L,d) = \frac{1}{N_s}\sum_{i=1}^{N_s}\left[\left(\sum_Y w_Y\right)^{-1}\sum_Y w_Y\left(\frac{a_{Y(\mathrm{cal})} - a_{Y(\mathrm{exp})}}{a_{Y(\mathrm{exp})}}\right)^2\right] \tag{20}$$

where the outermost sum runs over the N_s samples with different molecular weight and the innermost sum runs over the available properties for each sample. The advantage of using ratios of radii is that the a_Y are different but of the same order of magnitude, and in this way the properties are given a similar importance. Furthermore, the target function uses relative deviations, $[a_Y(\mathrm{cal}) - a_Y(\mathrm{exp})]/a_Y(\mathrm{exp})$. The user of Multi-HYDFIT could optionally use different weights w_Y for the various properties for specific purposes—for instance, to weight the properties according to their experimental precision. Note that Δ^2 is a mean-square relative deviation for a set of data; thus, 100Δ can be regarded as a typical difference between the calculated and experimental values for the whole set of properties of the series of samples. A bootstrap simulation is carried out to ascertain the uncertainty in the resulting parameters from some estimation of experimental errors of the data. For more details and examples of this strategy, see the original ref 22.

DNA: From 8 to 200 000 Base Pairs. Owing to its obvious relevance, and the continuous flexibility of the double helix, DNA is the paradigmatic application of the wormlike chain model. The bending flexibility of the double helix, measured by the persistence length, a, is of essential importance for many aspects of DNA function, and solution properties are a classical and still preferential source for its determination. The mass per unit length, M_L, and the diameter d are also fundamental structural parameters of the double helix. M_L is usually estimated directly from the geometry of the B-DNA helix, with a rise per base pair of 0.34 nm. The average molecular weight of base pairs of sodium−DNA is 660 Da, and this gives the commonly assumed value of M_L = 1950 Da/nm. Marginally, we recall that the average mass of base pairs in DNA is 616 Da[50,51] so that, if sodium ions are not fully condensed onto the DNA, M_L could be a little smaller. The diameter, d, of a cylindrical hydrodynamic model of DNA is not so predictable from the geometry of the helix, and it must have an important contribution from hydration. Thus, d, along with a are the parameters sought in the analysis of solution properties of DNA.

For many years, many authors have determined solution properties of DNA with the aim of determining those fundamental parameters. The techniques and samples studied have ranged from viscoelasticity of very long DNAs, like T2 DNA, with $M = 1.2 \times 10^8$ Da and about 200 000 base pairs,[52] to diffusion of oligomers with as few as 8 base pairs.[53] A commonly accepted value of the persistence length of DNA is $a \approx 50$ nm, although this figure is somehow a round number. The estimation of the diameter has yielded values in the range d = 2.0−2.5 nm. For short, rodlike oligonucleotides, whose properties do not depend on a, a precise estimation (based data for a number of diffusion data of oligonucleotides) is d = 2.3 nm.[54]

The progress in this knowledge of the wormlike model parameters of DNA has been slow and difficult (as it can be appreciated in the two monographs by Bloomfield, Crothers, and Tinoco[3,4]). Difficulties in the measurement (of light scattering, for instance) and even in the handling long DNAs, polydispersity in the early preparations of small or medium size samples and deficiencies or limited validity of theories have contributed to such long and slow progress. The presently accepted wormlike model parameters of DNA came from a number of scattered, diverse works in which some (usually one) solution properties were measured in a limited range of molecular weights. Thus, work in the 1970s fixed the presently accepted value of a, which had been overestimated earlier, but still overestimated the hydrated diameter, whose precise value was set more recently, thanks to the availability of measurements on very short DNA pieces (for which, as mentioned above, the hydrodynamics depends more strongly on the diameter) of exactly known length.[53−55]

In this work we show how the precise determination of the DNA wormlike parameters is feasible in a simple, efficient, and comprehensive manner, thanks to our new simulation results, implemented in the global analysis program Multi-HYDFIT. We analyze simultaneously data for four properties, R_g, D_t, s, and $[\eta]$. To do so, we have first made a compilation of data of solution properties of DNA which may be the most comprehensive one up to date, including samples ranging in length in the above-mentioned, extensive range, from an oligonucleotide of only 8 base pairs, to T2 DNA which has nearly 2×10^5 base pairs (the largest/smallest size ratio is ≈2500, i.e., over 4 decades). The experimental values are reported in the Supporting Information. We have collected and employed in the Multi-HYDFIT analysis 147 property−molecular weight data points, including 27 for R_g, 23 for D_t, 56 for s, and 41 for $[\eta]$. The data come from 41

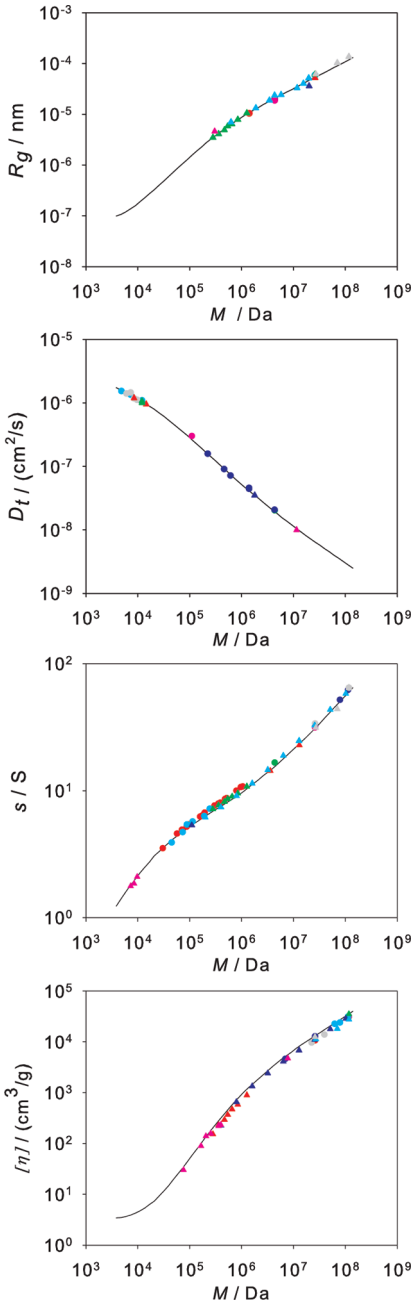

Figure 3. Plots of the experimental and calculated values, with a = 56 nm, d = 2.3 nm, and M_L = 1950 Da nm^{-1} for the four properties of DNAs.

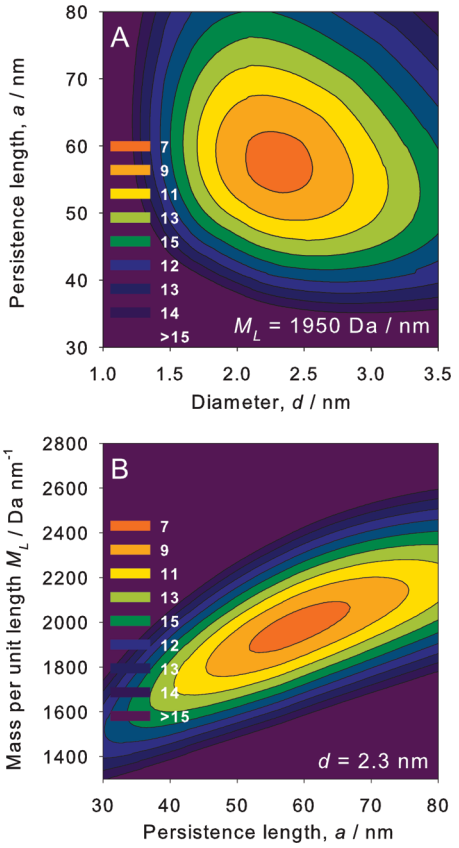

Figure 4. Contour plots of the percent typical deviation, 100Δ for DNA: (A) with fixed M_L = 1950 Da nm^{-1}; (B) with fixed d = 2.3 nm.

literature references, which are listed in the Supporting Information.

With the 147 data points as input, a single execution of the Multi-HYDFIT program gives immediately the three wormlike chain parameters of DNA: $a = 56 \pm 2$ nm, $d = 2.3 \pm 0.1$ nm, and $M_L = 1950 \pm 40$ Da/nm, with a typical percent deviation $100\Delta = 6.6\%$, which indicates an excellent overall reproduction of the 147 experimental values, as it is clearly visualized in Figure 3. The only remarkable feature is the slight upward deviation in the intrinsic viscosity. We recall that Multi-HYDFIT makes a simultaneous global fit of the four properties, and the quality of the fit may vary from one to another. Particularly, this may happen for the intrinsic viscosity because of its well-known larger sensitivity to structural details. Nonetheless, we note in Figure 3 how the log−log property vs M predicted curves of all the properties follow the changes in local slope (the so-called scaling exponents) depending on the molecular weight range, from the limit of rigid rod to that of the fully flexible chain with excluded volume. Enlarged views of these plots, including legends for the source of the experimental data, are presented in the Supporting Information.

The uncertainty of the fitted parameters reported by Multi-HYDFIT in the main results file is that of the position of the absolute minimum of the target function, resulting from the above-mentioned bootstrap simulation. But the program also reports a list of values of the target function over the whole ranges of the parameters. From this, an even more realistic impression of the sensitivity of the fit to each parameter can be grasped from the dependence of Δ on a, M_L, and d. This is illustrated by means of contour plots like those in Figure 4. Raising slightly the tolerance in the percent deviation, just to 7% ($\Delta < 0.07$), we note that there is a range of values of the parameters that fit the data nearly so well, a = 52−60 nm, d = 2.2−2.6 nm, and M_L = 1850−2050 nm. The above-mentioned, expected values of the parameters fall well within these ranges. A list of (a, M_L, d) sets giving $\Delta = 0.065-0.070$ is displayed in the Supporting Information.

In summary, we have been able to fit the wormlike chain parameters of DNA and predict its solution properties, R_g, D_t, s, and $[\eta]$ (with an error which is within typical experimental uncertainties), in a range covering about 4 decades in molecular weight, with a single (the same in the whole range) computational

dx.doi.org/10.1021/ma102697q |*Macromolecules* 2011, 44, 5788–5797

Table 2. Summary of the Results for All Polymers

	M/Da	a/nm	M_L/Da nm^{-1}	d/nm	100Δ	L/a	n_g	n_s	n_d	n_v	n_{tot}
DNA	6.0×10^3–1.2×10^8	56	1950	2.3	6.6	0.6–1100	27	23	56	41	147
schizophyllan	9.6×10^4–5.7×10^6	150	2050	2.3	4.2	0.3–18	11	11		22	44
poly(*n*-hexyl isocyanate)	6.8×10^4–5.5×10^6	37	645	1.0	6.7	2.8–230	26	19		25	70
poly(isobutylene)	5.5×10^2–5.5×10^6	0.71	205	0.69	6.2	0.8–38 500	17		13	27	57

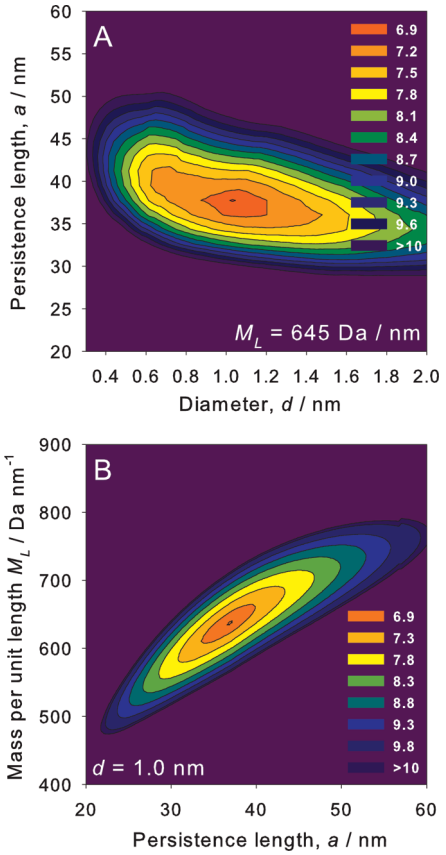

Figure 5. Contour plots of the percent typical deviation, 100Δ for PHIC: (A) with fixed M_L = 645 Da nm^{-1}; (B) with fixed d = 1.0 nm.

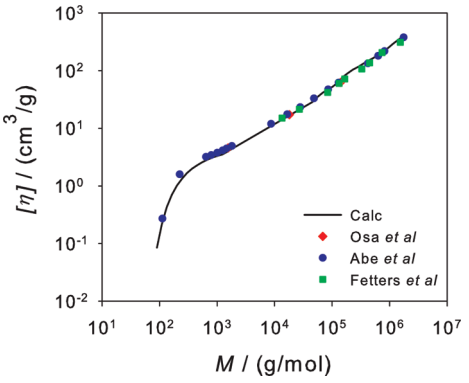

Figure 6. Plot of the experimental and calculated values for the intrinsic viscosity of PIB.

scheme derived from our new Monte Carlo simulation and in a single, and simple, execution of the Multi-HYDFIT global analysis tool.

Other Polymers. Because of the broad generality of the wormlike chain model, our methodology is applicable to virtually any linear polymer, including those in fully flexible, random coil conformations. In order to provide examples, additional to that of DNA, we have analyzed data of other stiff and flexible, natural, and synthetic polymers. A summary of the results is presented in Table 2. Below, we comment on the most salient features, and full results for each polymer are presented in the Supporting Information.

Schizophyllan is a fungal polysaccharide that has the remarkable structural feature of forming a triple-stranded helix, which makes it quite thick and remarkably stiff. Experimental data are taken from refs 30 and 56. The results, listed in Table 2, indicate that this polysaccharide has a diameter and a mass per unit length similar to that of DNA, and its extraordinary persistence length, a = 150 nm, is 3 times larger than that of DNA. The range of contour-to-persistence lengths corresponds to rigid to semiflexible conformations. It is thanks to these remarkable values that schizophyllan is an excellent thickener, i.e., viscosity intensifier, for aqueous systems (intrinsic viscosity $[\eta]$ = 12 000 cm^3/g for $M = 5.7 \times 10^6$ Da). This along with its immunoestimulant properties makes it very useful for food and pharma formulations.

Poly(n-hexyl isocyanate) (PHIC). While a majority of synthetic polymers—including mainly vinyl polymers like poly(isobutylene), as described below—are essentially flexible, there are some others whose conformation is better represented by the intermediate range of the wormlike coil. This is the case of PHIC, which in addition to larger chain rigidity due to the −CO−NR group, may present an additional contribution to the overall stiffness due to the bulky side chain (R is *n*-hexyl in PHIC). We have employed our global wormlike model fitting approach to experimental data for solution properties of PHIC in *n*-hexane at 25 °C, mainly those reported for R_g, s, and $[\eta]$ by Murakami et al.[57] and also including, jointly, some earlier (slightly discrepant) results form Rubingh and Yu.[58] The results and optimum values are listed in Table 2, with a satisfactory quality of fit: 6.7% with data from both references,[57,58] 3.8% only with the data from Murakami et al.[57] The precision of the fit is also well illustrated by the contour plots in Figure 5.

Poly(isobutylene) (PIB). Now, as an extreme case of synthetic polymers with a very flexible chain, we consider PIB, taking experimental data of solution properties in *n*-heptane at 25 °C, from refs 59–62. Yamakawa and co-workers (see for instance ref 63) claimed that other vinyl polymers like poly(styrene) or poly(methyl methacrylate), because of tacticity, could require a more sophisticated model, the helical, torsioned wormlike chain; others like PIB and schizophyllan would not have such torsional contribution. So, considering that it is free from such eventual complication, we have taken PIB as representative of the fully flexible coil limit of the wormlike chain. Data from the above-mentioned references have been subjected to the Multi-HYDFIT

dx.doi.org/10.1021/ma102697q |*Macromolecules* 2011, 44, 5788–5797

analysis with the results reported in Table 2. We note that the highest molecular weights are in the limit of (extremely) long and flexible chain ($L/a = 3.8 \times 10^5$), while still the smallest oligomers can be well described by the fit, with the pronounced decrease in intrinsic viscosity of the smallest sample, illustrated in Figure 6, which also shows how our treatment reproduces, at the same time, the slope of about 0.65 in the log−log plot of $[\eta]$ vs M at high M's, thanks to the adequate inclusion of excluded-volume effect in our treatment.

DISCUSSION AND CONCLUDING REMARKS

Comparing the results of our simulations with those of other theories and computational approaches, we note that the outcome depends on the range of parameters of the system under consideration. Thus, for the DNA parameters, $d \approx 2.3$ nm, $a \approx 56$ nm, and $M_L \approx 1950$ Da/nm, we find a very good agreement between our Monte Carlo calculation and the results of the path integration approach[20] within the limited range covered by the latter (70−6000 base pairs); the root-mean-square percent differences in radius of gyration and the two hydrodynamic properties is about 7%. This good agreement between the two approaches confirms the validity of each other. When comparing with the classical Yamakawa−Fujii (YF) theory,[7−9] we find that, in spite of its well-known approximate character (mainly regarding the preaveraging approximation), the validity within its range for DNA is quite acceptable, even for the longest DNAs, that are covered by their theory as well as by our calculation. The deviations remain quite low for short DNA and increase slightly with chain length, up to, for instance, 15% in the case of the translational radius for the longest DNA. The preaveraging approximation in the Yamakawa−Fujii theory produces an overestimation of the hydrodynamic radii, while the neglect of the excluded volume produces the contrary effect; thus, the good performance may be due to a cancelation of effects.

For a different range of the model parameters, the comparison may have a different outcome (full results are reported in Figures S-9 and S-10 of the Supporting Information). In the limit of very flexible chains, the wormlike chain model would cover from typically wormlike oligomers to fully flexible random coils. The latter are usually measured in good solvents, and excluded volume effects are essential. Our treatment combines chain stiffness and excluded volume, and thus it is able to predict the properties of very flexible polymer chains. The extremely wide range of applicability of our treatment, regarding both the variety of polymers to which it is applicable and the range of molecular weight, covering cases having from 0.6 up to 3×10^4 persistence lengths, is demonstrated in Table 2.

We must note that in our work we have not considered explicitly intramolecular interactions arising from electrostatic repulsions, proper of polyelectrolyte effects. The results can be safely applied to nonionic macromolecules and uncharged particles (like the nonionic schizophyllan polysaccharide or the synthetic polymers PHIC or PIB). Application to polyelectrolytes should be made only in conditions where high ionic strength, I, is sufficiently high as to shield the electrostatic repulsions (or with results extrapolated to $1/I \rightarrow 0$). An extension of our scheme to include electrostatic repulsions is feasible, using either Debye−Hückel treatments, or even simplified representations like that of an effective (expanded) hard-core diameter of the wormlike filament.[43−45] However, this would add one or more parameters to the three parameters that we are already considering, making simulations quite burdensome and the multiparameter fit of experimental data practically unviable.

Of the systems employed as examples in this work, the electrostatic repulsion should have some effect on the DNA of very high molecular weight. All kinds of excluded volume become appreciable when the contour length L is much higher than the Kuhn length; say $L/2a > 20$, or $M > \approx 5 \times 10^6$ for DNA; this would affect to a minor, final part of the wide range covered in our analysis. It is to be noted that, nonetheless, the quality of the fit is rather good even in that range, as it can be appreciated in Figure 3. Actually, all the 147 experimental values of solution properties of DNA correspond to ionic strength 0.1 M or higher (0.2 M in most cases, particularly for high M), at which most workers have assumed that electrostatic shielding in double-stranded DNA is complete and the wormlike model is applicable. There are however some indications that even at 0.2 M some appreciable electrostatic repulsion may take place.[43,64] This possibility is connected with our finding of persistence length, 56 nm, slightly higher than the customarily adopted value of 50 nm. There is another way of treating the joint effect of stiffness and electrostatics in the form of an apparent or effective persistence length which adds the electrostatic effect to the chain stiffness[65−67] and is valid at low or moderate ionic strength, when the Debye length is smaller than the persistence length.[68]

In conclusion, we remark that in the present paper we have presented (i) new calculations of the solution properties of wormlike molecules, covering the full range of parameters of the model, very short rigid cylinders to fully flexible chains, including excluded volume effects, and (ii) a systematic scheme, implemented in a computer program, for the determination of the three structural parameters—persistence length, a, diameter d, and mass per unit length, M_L—by fitting simultaneously experimental data of various solution properties. As examples of application we have described the solution properties, fitting the wormlike chain parameters of macromolecules with different degrees of stiffness over wide ranges of molecular weight. It is hoped that our results and the computational tools that we have developed will be useful to analyze solution properties of a variety of macromolecules and nanoparticles.

COMPUTER PROGRAMS

Program WORMCYL, which implements the results of our simulation in the calculation of the solution properties of any wormlike macromolecule, and a new version of program MultiHYDFIT, which fits the wormlike chain parameters by global analysis of various solution properties of a series of samples, can be freely downloaded from our Web site, http://leonardo.inf.um.es/macromol/.

ASSOCIATED CONTENT

Supporting Information. Tables and plots of the ratios of radii, R_G ratios, Q_∞, and α_G^2 parameters calculated from Monte Carlo for wormlike chains with and without excluded volume; tables and plots of the experimental properties, R_G, D_t, s, and $[\eta]$ of DNA fragments from different authors and plots of the calculated properties for these fragment lengths; table showing the set of parameters for DNA that shows a $100\Delta < 7\%$; plots of calculated and experimental properties for different semiflexible polymers; plots showing a comparison of the different theories available for the calculation of properties of wormlike chains.

This material is available free of charge via the Internet at http://pubs.acs.org.

AUTHOR INFORMATION

Corresponding Author
*E-mail: jgt@um.es.

ACKNOWLEDGMENT

This work was performed within a Grupo de Excelencia de la Región de Murcia (grant 04531/GERM/06). Support also provided by grant CTQ-2009-08030 from Ministerio de Ciencia e Innovación (MICINN), including FEDER funds. A.O. acknowledges a postdoctoral fellowship from Universidad de Murcia, and D.A. is recipient of a predoctoral fellowship from MICINN. Computing time and support were provided by Parque Cientfico de Murcia in the Ben Arabi SuperComputer.

REFERENCES

(1) Kratky, O.; Porod, G. *Recl. Trav. Chim. Pays-Bas* **1949**, *68*, 1106–1122.
(2) McNaught, A. D.; Wilkinson, A. *Compendium of Chemical Terminology. The Gold Book*, 2nd ed.; Blackwell Science: London, 1997.
(3) Bloomfield, V.; Crothers, D.; Tinoco, I. *Physical Chemistry of Nucleic Acids*; Harper and Row: New York, 1974.
(4) Bloomfield, V.; Crothers, D.; Tinoco Jr., I. *Nucleic Acids: Structures, Properties and Functions*; University Science Books: Sausalito, CA, 2000.
(5) Sho, T.; Sato, T.; Norisuye, T. *Biophys. Chem.* **1986**, *25*, 307–313.
(6) Harding, S.; Berth, G.; Ball, A.; Mitchell, J.; García de la Torre, J. *Carbohydr. Polym.* **1991**, *16*, 1–15.
(7) Yamakawa, H.; Fujii, M. *J. Chem. Phys.* **1973**, *6*, 408–414.
(8) Yamakawa, H.; Fujii, M. *Macromolecules* **1974**, *7*, 128–135.
(9) Yamakawa, H.; Fujii, M. *Macromolecules* **1974**, *7*, 649–654.
(10) García de la Torre, J.; López Martínez, M.; Tirado, M.; Freire, J. *Macromolecules* **1983**, *16*, 1121–1127.
(11) García de la Torre, J.; López Martínez, M.; Tirado, M.; Freire, J. *Macromolecules* **1984**, *17*, 2715–2722.
(12) Zimm, B. *Macromolecules* **1980**, *13*, 592–602.
(13) Hagerman, P.; Zimm, B. *Biopolymers* **1981**, *20*, 1481–1502.
(14) García de la Torre, J.; Jiménez, A.; Freire, J. *Macromolecules* **1982**, *15*, 148–154.
(15) Kirkwood, J.; Riseman, J. *J. Chem. Phys.* **1948**, *16*, 565–573.
(16) García de la Torre, J.; Bloomfield, V. *Q. Rev. Biophys.* **1981**, *14*, 81–139.
(17) García Bernal, J.; Tirado, M.; Freire, J.; García de la Torre, J. *Macromolecules* **1990**, *23*, 3357–3362.
(18) García Bernal, J.; Tirado, M.; García de la Torre, J. *Macromolecules* **1991**, *24*, 593–598.
(19) García Molina, J.; López Martínez, M. C.; García de la Torre, J. *Biopolymers* **1990**, *29*, 883–900.
(20) Mansfield, M. L.; Douglas, J. F. *Macromolecules* **2008**, *41*, 5412–5421.
(21) García de la Torre, J.; Del Río Echenique, G.; Ortega, A. *J. Phys. Chem. B* **2007**, *111*, 955–961.
(22) Ortega, A.; García de la Torre, J. *Biomacromolecules* **2007**, *8*, 2464–2475.
(23) Benoit, H.; Doty, P. *J. Phys. Chem.* **1953**, *57*, 958–963.
(24) Carrasco, B.; García de la Torre, J. *Biophys. J.* **1999**, *76*, 3044–3057.
(25) Carrasco, B.; García de la Torre, J. *J. Chem. Phys.* **1999**, *111*, 4817–4826.
(26) Ortega, A.; García de la Torre, J. *J. Am. Chem. Soc.* **2005**, *127*, 12764–12765.
(27) García de la Torre, J.; Amorós, D.; Ortega, A. *Eur. Biophys. J.* **2010**, *39*, 381–388.
(28) Schellman, J. *Biophys. Chem.* **1980**, *11*, 329–337.
(29) Flory, P. *Statistical Mechanics of Chain Molecules*; Interscience: New York, 1969.
(30) Yanaki, T.; Norisuye, T.; Fujita, H. *Macromolecules* **1980**, *13*, 1462–1465.
(31) Huber, K.; Burchard, A. A., W. *Macromolecules* **1985**, *18*, 2743–2747.
(32) Einaga, Y.; Koyama, H.; Konishi, T.; Yamakawa, H. *Macromolecules* **1989**, *22*, 3419–3424.
(33) Ortega, A.; García de la Torre, J. *J. Chem. Phys.* **2003**, *119*, 9914–9919.
(34) Youngren, G.; Acrivos, A. *J. Fluid Mech.* **1975**, *69*, 377–403.
(35) Yamakawa, H. *Macromolecules* **1975**, *8*, 339–342.
(36) Yoshizaki, T.; Yamakawa, H. *J. Chem. Phys.* **1980**, *72*, 57–79.
(37) Bonet Avalos, J.; Rubí, J.; Bedeaux, D. *Macromolecules* **1993**, *26*, 2550–2561.
(38) Flory, P.; T. G., F., Jr. *J. Am. Chem. Soc.* **1951**, *73*, 1904–1908.
(39) Flory, P. *Principles of Polymer Chemistry*; Cornell University Press: Ithaca, NY, 1953.
(40) Miyaki, Y.; Einaga, Y.; Fujita, H.; Fukuda, M. *Macromolecules* **1980**, *13*, 588–592.
(41) Schmidt, M.; Burchard, W. *Macromolecules* **1981**, *14*, 210–211.
(42) Bohdanecky, M.; Petrus, V.; Porsch, B.; Sundelof, L. *Makromol. Chem.* **1983**, *184*, 309–317.
(43) Stigter, D. *Biopolymers* **1977**, *16*, 1435–1448.
(44) Vologodskii, A.; Cozzarelli, N. *Biopolymers* **1995**, *35*, 289–296.
(45) Rybenkov, V.; Vologodskii, A.; Cozzarelli, N. *Nucleic Acids Res.* **1997**, *25*, 1412–1418.
(46) Jamieson, A.; Venkataswamy, K. *Polym. Bull.* **1984**, *12*, 275–282.
(47) Venkataswamy, K.; Jamieson, A.; Petschek, R. *Macromolecules* **1986**, *19*, 124–133.
(48) LeGuillou, J. C.; Zinn-Justin, J. *Phys. Rev. Lett.* **1977**, *39*, 95–98.
(49) Rawiso, M.; Duplessix, R.; Picot, C. *Macromolecules* **1987**, *20*, 630–648.
(50) Muddiman, D.; Mull, A.; Hannis, J. *Rapid Commun. Mass Spectrom.* **1999**, *13*, 1201–1204.
(51) Dolozel, J.; Bartos, J.; Voglmayr, H.; Greilhuber, J. *Cytometry* **2003**, *51A*, 127–128.
(52) Bowen, B.; Zimm, B. *Biophys. Chem.* **1978**, *7*, 235–252.
(53) Eimer, W.; Williamson, J.; Boxer, S.; Pecora, R. *Biochemistry* **1990**, *29*, 799–811.
(54) Fernandes, M.; Ortega, A.; López Martínez, M.; García de la Torre, J. *Nucleic Acids Res.* **2002**, *30*, 1782–1788.
(55) Tirado, M.; López Martnez, M.; García de la Torre, J. *J. Chem. Phys.* **1984**, *81*, 2047–2052.
(56) Kashiwagi, Y.; Norisuye, T.; Fujita, H. *Macromolecules* **1981**, *14*, 1220–1225.
(57) Murakami, H.; Norisuye, T.; Fujita, H. *Macromolecules* **1980**, *13*, 345–352.
(58) Rubingh, D.; Yu, H. *Macromolecules* **1976**, *9*, 681–685.
(59) Abe, F.; Einaga, Y.; Yamakawa, H. *Macromolecules* **1993**, *26*, 1891–1897.
(60) Osa, M.; Abe, F.; Yoshizaki, T.; Einaga, Y.; Yamakawa, H. *Macromolecules* **1996**, *29*, 2302–2308.
(61) Yamada, M.; Osa, M.; Yoshizaki, T.; Yamakawa, H. *Macromolecules* **1997**, *30*, 7166–7170.
(62) Fetters, L. J.; Hadjichristidis, N.; Lindner, J. S.; Mays, J. W.; Wilson, W. W. *Macromolecules* **1991**, *24*, 3127–3135.
(63) Yamakawa, H. *Polym. J.* **1999**, *31*, 109–119.
(64) Stigter, D.; Dill, K. *J. Phys. Chem.* **1993**, *97*, 12995–12997.
(65) Odijk, T. *J. Polym. Sci., Part B: Polym. Phys.* **1977**, *15*, 477–483.
(66) Skolnick, J.; Fixman, M. *Macromolecules* **1977**, *10*, 944–948.
(67) Schmidt, M. *Macromolecules* **1991**, *24*, 5361–5364.
(68) Fixman, M. *J. Phys. Chem. B* **2010**, *114*, 3185–3196.